Measurement 158 (2020) 107682

Contents lists available at ScienceDirect

Measurement

journal homepage: www.elsevier.com/locate/measurement

3-D printed primary standards for calibration of microwave network analysers

Adam Jones [a], Stepan Lucyszyn [b], Enrique Márquez-Segura [c], Nick Ridler [a,*], James Skinner [a], Daniel Stokes [a]

[a] National Physical Laboratory (NPL), Hampton Road, Teddington TW11 0LW, UK
[b] Imperial College London, Exhibition Road, London SW7 2AZ, UK
[c] Universidad de Málaga, Av. de Cervantes, 2, 29016 Málaga, Spain

ARTICLE INFO

Article history:
Received 6 January 2020
Received in revised form 24 February 2020
Accepted 26 February 2020
Available online 3 March 2020

Keywords:
3-D printing
Additive manufacturing
Calibration
Measurement standards
Metrological traceability
Scattering parameters
Vector network analyser
VNA
Waveguide

ABSTRACT

This paper describes the design, fabrication and testing of 3-D printed primary standards for use with the calibration of microwave vector network analysers. The standards are a short-circuit and a quarter wavelength section of line that are designed for use with the Thru-Reflect-Line calibration technique. The standards are realised in metal-pipe rectangular waveguide, covering the frequency range from 12 GHz to 18 GHz (i.e., Ku-band). The standards are polymer-based 3-D printed, which is subsequently metal plated to provide the required electrical conductivity. The performance of the standards is compared with conventionally machined standards that are used as part of the UK's primary national measurement system for microwave scattering parameters. The authors believe that this is the first time that 3-D printing techniques have been used to produce such calibration standards, and, that this could lead to a new approach to providing metrological traceability for these types of measurement.

1. Introduction

Additive manufacturing using 3-D printing technology is becoming an established manufacturing technique for many different applications, impacting both everyday life and many areas of science and technology. One such area where 3-D printing technology has been used very successfully, in recent years, relates to the production of electronic components and systems operating at very high frequencies. Metal-pipe rectangular waveguide is often the preferred transmission medium, at these frequencies. Therefore, the reliable manufacture of high-quality waveguide is of the utmost importance to industrial sectors that use these very high frequencies (e.g., for telecommunications, security, defence, space, etc.).

3-D printing can be mainly classified as being either metal-based or polymer-based, both requiring additional metal plating. With the former, binder jetting/sintering and selective laser melting (SLM) can be adopted to build these high frequency waveguides. However, for many applications at these frequencies, metal-based 3-D printing has the disadvantage that, without non-trivial post-fabrication processing (e.g., additional metal plating), the internal waveguide sidewalls exhibit poor intrinsic conductivity and poor surface roughness; both contributing to poor electrical performance at these frequencies, due to elevated surface resistance. Nevertheless, such waveguides and associated horn antennas have been demonstrated [1,2].

In the past few years, much work has focussed on additive manufacturing using polymer-based 3-D printing for high frequency applications, including rectangular waveguides [3–12]. Polymer-based 3-D printing offers many advantages over metal-based 3-D printing, including having excellent internal wall intrinsic conductivity, low surface roughness and the possibility of realising entirely new designs for components and systems that were not previously possible using conventional subtractive manufacturing techniques. Rectangular waveguides have been manufactured using a variety of polymer-based 3-D printing technologies: fused deposition modelling (FDM) at X-band (8.2–12.4 GHz) [4], stereolithographic apparatus (SLA) at W-band (75–110 GHz) [4], polymer-jetting (Polyjet) in the WM-570 band (325–500 GHz) [11] and RECILS in the WM-380 band (500–750 GHz) and WM-250 band (750–1.1 THz) [10].

One application of 3-D printing that has yet to be explored is the production of artefact standards used in metrology. Since waveg-

* Corresponding author.
E-mail address: nick.ridler@npl.co.uk (N. Ridler).

https://doi.org/10.1016/j.measurement.2020.107682

uides are used routinely as standards for high frequency electromagnetic measurements, a potential application is to develop sets of 3-D printed waveguide standards and use these to calibrate, for example, vector network analysers (VNAs).

Another potential advantage with 3-D printing objects is that they can be produced by end-users, at end-user locations, (using a 3-D printer) as and when they are needed. This is in contrast to traditional manufacturing processes, where objects are produced by a supplier (e.g., manufacturer) and sent to customers (e.g., end-users) at various different end-user locations. In a metrology context, this means that artefact standards can be 3-D printed by (and at) end-user measurement laboratories. In certain circumstances, metrological traceability can then also be achieved at the end-user location. For example, in microwave network analysis, precision transmission lines and waveguides are used as standards in conjunction with the Thru-Reflect-Line (TRL) calibration technique [13]. Traceability for measurements made with reference to these standards can be achieved via traceable dimensional measurements of the standards (e.g., using local dimensional standards such as calibrated gauge blocks). Traceability can then be achieved at the end-user location using measurement software that can either be downloaded from, or accessed via, the internet [14–16]. This is in contrast to the traditional traceability route, whereby traceability is transferred from primary reference standards at national metrology institutes (NMIs) to end-users via a series of comparisons (e.g., by ISO/IEC 17025 accredited laboratories) using transfer standards. The use of 3-D printing, therefore, has the potential to be a disruptive technology for the process of providing metrological traceability.

In this paper, the design, manufacture and testing of a set of 3-D printed standards is described for use with the TRL VNA calibration technique in the 60153 IEC-R 140 waveguide band [17], which operates from 12 GHz to 18 GHz. This waveguide band is also known as Ku-band, J-band, WR-62 and WG-18. Ku-band will be used within this paper, as this term is currently used by many users of waveguides (this being the IEEE radar-frequency band letter designation [18]). The TRL calibration technique has the advantage that it is often used for both industry-level measurements (e.g. for product testing, etc) as well as for precision metrology applications (e.g. as used by NMIs to provide metrological traceability for microwave scattering (S-)parameter measurements).

Section 2 of the paper describes the process used to 3-D print the calibration standards. Section 3 presents the initial tests of the performance of the 3-D printed standards. Section 4 gives a comparison between two sets of microwave S-parameter measurements, calibrated with respect to the: (i) 3-D printed standards, and (ii) UK's existing primary national measurement standards, which were manufactured using conventional machining. Section 5 demonstrates the use of the 3-D printed standards using an instrument firmware calibration, as is often used for many end-user applications (e.g., in industry). Finally, Sections 6 and 7 provide a discussion on, and a summary of, all the work presented in this paper.

2. Fabrication details

Two calibration standards were manufactured to implement the TRL calibration technique in metal-pipe rectangular waveguide technology: a ¼ wavelength (¼-wave) line section and a flush (i.e., zero offset length) short-circuit. The length of the ¼-wave line was chosen to optimise the calibration (i.e. to provide a phase shift of a ¼ of a guided wavelength) in the middle of the waveguide band (i.e., *ca.* 15 GHz for Ku-band waveguide). The chosen length for the design of the line standard was therefore 6.4 mm. Both the ¼-wave line and short-circuit were manufactured using polymer-based 3-D printing.

Among several available 3-D printing technologies, the Polyjet process was chosen for the fabrication of the standards due to its high accuracy and smooth surface finish. The Polyjet process produces 3-D components by jetting drops of photopolymer resin onto the build plate, which is then cured using ultraviolet light [19]. The printer used was a Stratasys Connex3 Object260, which has a *z*-axis build resolution that equates to a minimum layer height of 16 μm, and, *x*- and *y*-axis bed resolution of 42 μm [20]. The material used in the fabrication process was Digital ABS Plus, from Stratasys, which exhibits high impact strength with high-temperature resistance and a heat deflection temperature of up to 95 ^{0}C. This material also has the advantage of a polymerised density of 1.18 g/cm^3 [21], which is approximately an 1/8 the density of metals such as brass, which is traditionally used in the fabrication of such components. The schematics used to produce the models for the 3-D printing process are shown in Fig. 1. The waveguides were 3-D printed at the University of Malaga, Spain, in a single batch. It was not necessary to produce multiple batches and to select the best components from these batches, or, to implement any kind of design/print iteration to obtain the necessary product quality.

The polymer-based waveguides were subsequently metallised to obtain the finished version of the two calibration standards. The metallisation, provided by JetMetal Technologies [22], was carried out using a direct plating procedure executed at a controlled room temperature and ambient pressure that allows the deposition of metallic films on plastic or composites. Digital ABS was metallised with a 2 μm thick layer of silver, which is almost four times the skin depth, δ, at the lowest frequency of operation ($\delta|_{12GHz} \approx 0.6$ μm). The metallisation is based on a sequential supply of silver (Ag^+) ions and a reducing agent using a double nozzle paint spraying gun. The thickness of the silver layer is controlled by monitoring the time allowed for the reaction, as this is a well understood process, dependent on a specific ambient temperature and pressure.

Fig. 2 shows photographs of the 3-D printed standards. These photographs were taken after the standards had been used for all the investigations reported in this paper. Fig. 2(a) shows the ¼-wave line, and Fig. 2(b) shows the short-circuit. For comparison, Fig. 3 shows equivalent items manufactured using conventional machining. These are the UK's existing primary national standards: Fig. 3(a) is the ¼-wave line and Fig. 3(b) is the short-circuit.

3. Preliminary assessments

Since the ¼-wave line standard is the only artefact standard in the TRL calibration process that is required to have well-defined electrical characteristics [13], a detailed assessment of this standard was carried out before using the line for VNA calibration. The initial assessment of the line standard involved undertaking a series of dimensional measurements, to determine the length and aperture size, made when the line was not connected to any test equipment. A micrometer and vernier caliper, both calibrated using gauge blocks with traceability to national length standards, were used to make these measurements.

The dimensional measurements of the line's length was used to predict the transmission phase for the line. These predicted values were compared with electrically-determined values of transmission phase, measured using a VNA. The dimensional measurements of the line's aperture size were used to determine the uncertainty contribution from the line when it is used as a standard for a TRL calibration of a VNA.

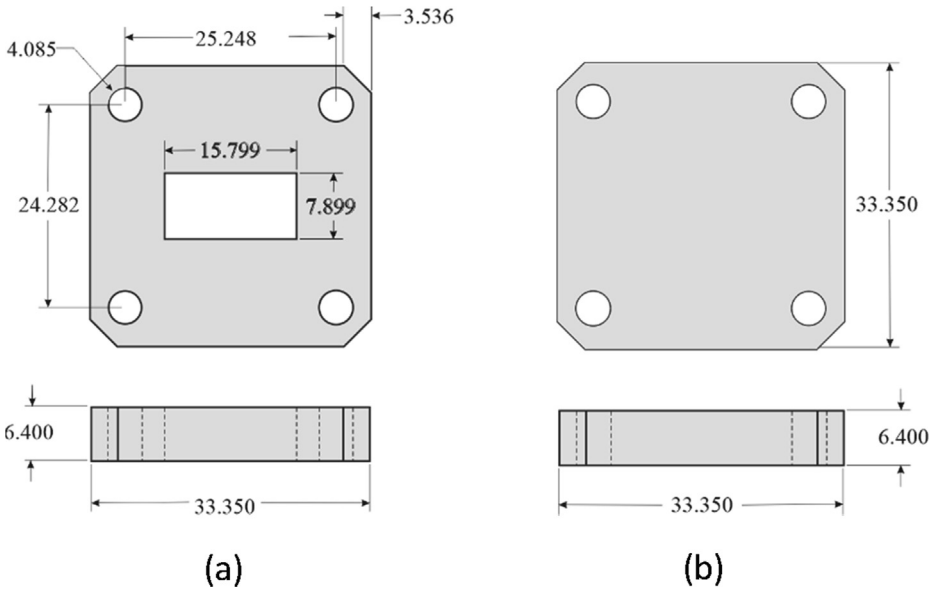

Fig. 1. Engineering drawings showing the dimensions of the two Ku-band waveguide calibration standards: (a) ¼-wave line; and (b) short-circuit. All dimensions are in millimetres.

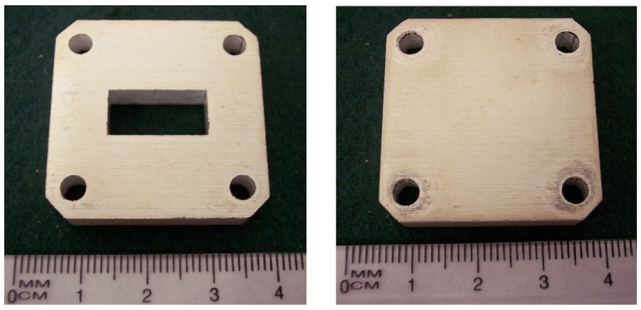

Fig. 2. Photographs of the 3-D printed standards: (a) ¼-wave line; and (b) short-circuit.

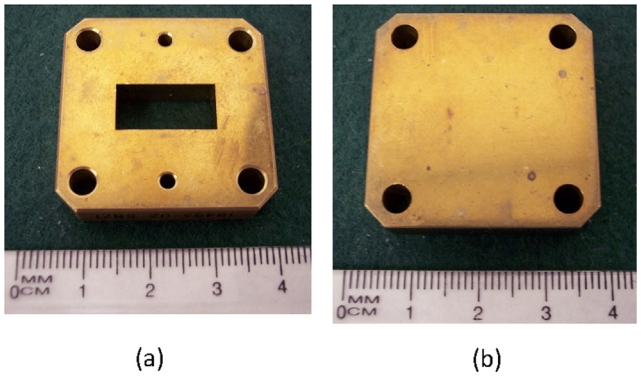

Fig. 3. Photographs of the UK's primary national measurement standards: (a) ¼-wave line; and (b) short-circuit.

Finally, some preliminary electrical measurements were made on the line and short-circuit, *in-operando* (i.e., when connected to the test ports of a VNA). These measurements were intended to detect any significant change in the line or short-circuit's electrical performance during operation. Although the short-circuit standard does not need to have well-defined electrical characteristics, when employed as the reflect standard in the TRL calibration process, it does need to provide the same value of reflection when connected to each of the two VNA's test ports [13] and without any radiation leakage at the flange interface.

3.1. Line – length

Six repeat measurements of the length of the line were made using a micrometer at different locations on the face of the waveguide flanges. The mean measured length was found to be 6.408 mm, and the standard deviation in the mean was 3 μm. This Type-A standard uncertainty [23] gives an indication of the manufacturing quality of the line (i.e., indicating variations in the line's length and surface finish of the waveguide flange faces, both due to manufacturing process variations). For comparison, a similar set of measurements were made on a high precision metal line (i.e., the line that is used as the UK's primary national standard for this waveguide size), which was manufactured using conventional machining techniques. The standard uncertainty in the repeat measurements of the length of the metal line was found to be 1 μm. Unsurprisingly, this shows that the flatness of the surfaces on the 3-D printed line is not quite as good as the conventionally manufactured line (i.e., the UK national standard). However, the uncertainty (due to the micrometer accuracy) in all these measurements is expected to be of the order of 5 μm, and so the variation in these line length measurements, as represented by the Type-A standard uncertainty (i.e., 3 μm for the 3-D printed waveguide and 1 μm for the machined waveguide), is not considered significant in the context of the overall uncertainty in these micrometer measurements. The uncertainty of 3 μm in the measured length of the 3-D printed waveguide is approximately twice the minimum layer height given in the printer specification [20].

The mean measured length of the 3-D printed line was used to predict the transmission phase for the line. This predicted phase was then compared with transmission phase measurements made using a VNA. The VNA was calibrated using a TRL calibration using the UK's primary national standards. The predicted transmission phase, $\phi(f)$, for a line of length, l, at frequency, f, is given by:

$$\phi(f) = -360\left(\frac{l}{\lambda_g(f)}\right) \quad (1)$$

where $\lambda_g(f)$ is the guide wavelength, given by:

$$\lambda_g(f) = \frac{\lambda(f)}{\sqrt{1-(\lambda(f)/\lambda_c)^2}} \quad (2)$$

where $\lambda(f)$ is the free-space wavelength and λ_c is the cut-off wavelength of the waveguide, which is defined as:

$$\lambda_c = 2a \quad (3)$$

where a is the broad wall dimension of the waveguide aperture. For Ku-band waveguide, the nominal broad wall dimension is 15.799 mm [17] and so according to equation (3), $\lambda_c = 2 \times 15.799 = 31.598$ mm.

The free space wavelength, λ, is given by:

$$\lambda(f) = \frac{v}{f} \quad (3)$$

where v is the speed of the electromagnetic wave, given by:

$$v = \frac{c}{\sqrt{\varepsilon_r}} \quad (4)$$

where c is the speed of light in vacuum (defined as 299 792 458 m/s) and ε_r is the relative permittivity of air (assumed here to be 1.000 649, as this value is appropriate for 'standard' air at 23 °C, 50% relative humidity and 1013.25 mbar atmospheric pressure [24], which are the environmental conditions within the laboratory where this investigation took place).

Fig. 4(a) shows a plot of the predicted and measured transmission phase for the 3-D printed waveguide. This plot shows that the predicted and measured phase are very similar (i.e., the two traces overlap each other). Fig. 4(b) shows a plot of the difference between the predicted and measured phase in Fig. 4(a). All phase differences are less than 0.2° across the full waveguide band. This is equivalent to an average discrepancy between an electrical and mechanical determination of line length of approximately 5 μm. This is a similar level of agreement to that observed for a conventionally machined line where this discrepancy is typically 2 μm. Fig. 4(b) also plots the uncertainty in the phase measurements, which shows that the phase differences are less than the uncertainties at all frequencies. These phase differences are therefore considered to be insignificant, in the context of this uncertainty. The main sources of uncertainty in the VNA's phase measurements are random errors due to connection repeatability and length errors in the calibration standards. The relationship between this uncertainty and the measured phase difference is not expected to be significant.

3.2. Line – aperture size

Repeat measurements of the broad and narrow wall dimensions of the waveguide aperture were made using a vernier calliper at various positions across the width and height of the waveguide apertures. For each aperture, four measurements were made of the broad wall dimension and eight measurements were made of the narrow wall dimension. These measurements are summarised in Table 1, in terms of the overall mean measured value (for both apertures) and associated standard deviation in the mean (i.e., Type-A standard uncertainty [23]).

The nominal aperture dimensions for this waveguide size are 15.799 mm × 7.899 mm. These are used to specify the CAD model used in the 3-D printing process. Imperfections in the printing and plating processes give rise to deviations in the dimensions from these nominal values.

Deviations from the nominal dimensions, or misalignment when connecting the line to the VNA test ports, will cause the line standard to produce reflections that will impact the quality of the TRL calibration that, in turn, will impart some degree of error in subsequent measurements made using the calibrated VNA. This source of error is included in the uncertainty budget used within NPL's Primary Impedance Microwave Measurement System (PIMMS) [25]. The deviations from nominal in the measured broad wall and narrow wall dimensions of the 3-D printed line are −14 μm and + 2 μm, respectively, which is much less than the printer resolution of 42 μm [20]. By comparison, deviations between actual and nominal dimensions for conventionally machined high precision waveguides of this size are expected to be within 5 μm.

A close look at the 3-D printed line, as shown in Fig. 2(a), indicates that the printing process can produce minor defects on the waveguide walls and on the face of the waveguide flanges. However, these defects are small and considered insignificant for this waveguide size. However, the impact of such defects will become more significant for smaller waveguide sizes that are needed at higher frequencies (e.g., at millimetre wavelengths).

3.3. Line – in-operando

Recognising that these 3-D printed components are manufactured using a silver-plated solid polymer that may still be compressible, to some extent, an important consideration is the behaviour of the 3-D printed line, *in-operando*. This is important

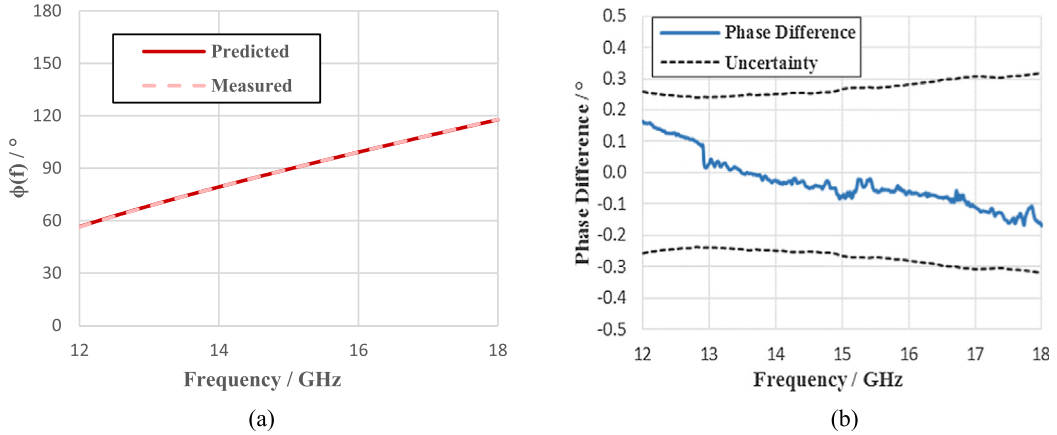

Fig. 4. (a) Predicted and measured transmission phase for the 3-D printed line: (b) difference between predicted and measured transmission phase.

Table 1
Waveguide aperture measurements.

Dimension	Nominal value (mm)	Mean measured value (mm)	Type-A standard uncertainty (mm)	Deviation from nominal (mm)
Broad wall	15.799	15.785	0.006	−0.014
Narrow wall	7.899	7.901	0.018	+0.002

because the line's length may change due to compression caused by the pressure applied to each waveguide flange during connection. This behaviour was investigated by connecting the 3-D printed line to the test ports of the VNA, leaving it connected, and taking a measurement of transmission phase every minute, for 10 minutes. A change in the length of the waveguide after connection to the VNA will cause an associated change in the relative phase of the voltage-wave transmission coefficient (VTC).

Fig. 5 shows the measurement results obtained at 15 GHz; other frequencies showed a similar behaviour. The results are presented as a change in transmission phase, relative to the first measurement made after connecting the line to the VNA. The change in VTC phase is less than 0.1° at 15 GHz, which is equivalent to a change in length of less than 7 μm. This phase change is relatively small compared to the uncertainty in such a measurement, which is typically 0.25°. In addition, the change in phase could also be attributed, to some extent, to drift in the measurement system (e.g. due to flexing of the cables that are used to connect the VNA to the waveguide). By comparison, the change in VTC phase observed whilst measuring the UK's primary national standard line over the same period of time was found to be of a similar amount (i.e., less than 0.1° at 15 GHz). This suggests that any *in-operando* change in length of the 3-D printed line will not be significant in the context of a VNA calibrated using the line as a standard.

3.4. Short-circuit – in-operando

During the TRL calibration process, the short-circuit is used as the reflect standard. As such, although the value of the reflection for the short-circuit does not need to be known, it does need to provide the same value of reflection (to within the experimental error) when connected to each of the VNA's test port reference planes [13]. Therefore, to test the performance of the 3-D printed short-circuit, its voltage-wave reflection coefficient (VRC) was measured using both test ports of the calibrated VNA. The results obtained from both measurements are shown in Fig. 6(a), in terms of the linear magnitude of the VRC. (Since the short-circuit contains no offset length, the phase of the VRC will be 180°, to within the experimental error.)

Fig. 6(a) shows that the measurements of the VRC linear magnitude for the 3-D printed short-circuit, made using both the VNA test ports, agree to within 0.002. This is similar to the level of agreement found for a conventionally manufactured short-circuit, when measured using both VNA test ports, as shown in Fig. 6(b). This level of agreement is also less than the typical uncertainty for such a measurement (which is of the order of 0.004). This demonstrates that the 3-D printed short-circuit will provide acceptable electrical performance when used as the reflect standard during the TRL calibration process.

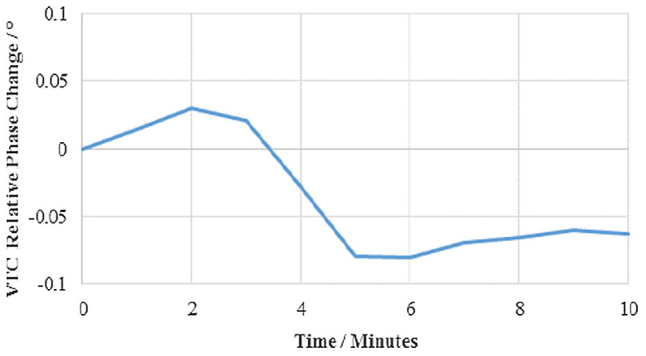

Fig. 5. Change in VTC phase, measured at 15 GHz, relative to the VTC phase measured immediately after connecting the 3-D printed waveguide to the VNA.

The measured VRC linear magnitude shown in Fig. 6(a) and (b) include some values that are greater than unity. Although it is theoretically not possible for the true value of the VRC linear magnitude of a passive component to exceed unity, in practice, such measured values can sometimes occur for high-reflecting components (i.e., where the true value of the VRC linear magnitude is very close to one); due to inherent measurement error. If this error is positive, the measured value will be greater than the true value, which can result in measured values greater than unity. However, this obvious error in the measured value (which implies nonphysical behaviour for the short-circuit) is less than the uncertainty in the measured value and so this justifies the validity of such a measured value. For the measurements presented in Fig. 6(a) and 6(b), the maximum measured VRC linear magnitude is approximately 1.002, while the typical uncertainty for this measurement is 0.004.

4. National standard comparison

Having verified the quality of the 3-D printed standards, a detailed comparison was undertaken between the UK's existing primary national measurement standards and the 3-D printed standards described in this paper. The comparison was based on using the standards to calibrate a VNA as part of PIMMS [25]. NPL uses PIMMS to provide metrological traceability for S-parameter measurements at the very highest levels of accuracy. As such, PIMMS provides the UK's contribution to the Calibration and Measurement Capabilities (CMCs) listed in the International Bureau of Weights and Measures (BIPM) key comparison database (KCDB) [26] for S-parameter measurements, which includes the UK's CMCs that are listed on the KCDB for S-parameter measurements in Ku-band waveguide (referred to as R 140 waveguide, in the KCDB). This demonstrates the international equivalence of these measurements via the International Committee of Weights and Measures (CIPM) Mutual Recognition Arrangement (MRA) [27]. NPL has used PIMMS for more than 25 years to provide end-user laboratories, including other NMIs from around the world, with traceability for S-parameter (both VRC and VTC) measurements.

PIMMS uses a VNA in conjunction with a TRL calibration for which the required standards are a length (typically, a ¼ wavelength) of precision transmission line/waveguide and a short-circuit. PIMMS also evaluates the uncertainties in the S-parameter measurements, following international recommendations [23] that have been adapted to account for the fact that S-parameters are complex-valued quantities [28,29]. PIMMS evaluates the uncertainty by considering both prior knowledge and information gathered during the measurement process used to collect data for the DUTs. The combination of these two sources of information establishes the overall uncertainty in the measurements. The prior knowledge relates to information about the measurement system (e.g. VNA linearity, noise floor, cross-talk

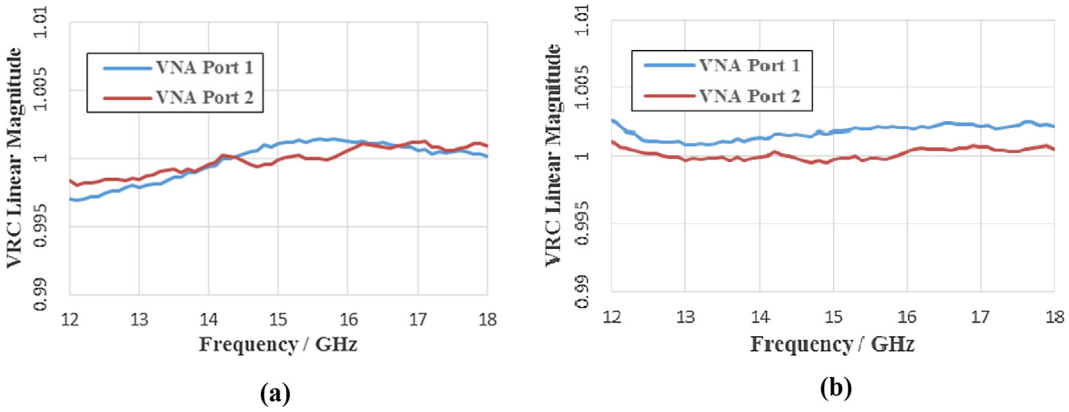

Fig. 6. VRC linear magnitude measured using the two VNA test ports: (a) 3-D printed short-circuit; (b) conventionally machined short-circuit.

isolation, etc.). The information gathered during the measurement process consists of repeated calibrations and measurements to assess the overall variability in the measurements (i.e., due to the connection repeatability of the calibration standards and the devices under test (DUTs), flexing of any cables that connect to the VNA, and, fluctuations in the ambient laboratory conditions – temperature, relative humidity, etc.).

The comparison was in two stages: first, PIMMS was calibrated using the UK's existing primary national standards and a set of measurements were made on a selection of DUTs, following normal operating procedures; second, PIMMS was calibrated using the 3-D printed standards and a second set of measurements were made on the same DUTs following the same operating procedures. By following this approach, the only difference between the two sets of measurements was the standards that were used for the measurements – i.e., in the first instance, these were the UK's primary national standards; in the second instance, these were the 3-D printed standards described in this paper. This meant that a direct comparison could be made between the performance (as primary reference standards, at the NMI level) of the 3-D printed standards and the UK's existing primary national standards, by examining differences in the measured S-parameters (VRC and VTC) of the DUTs made with respect to the two sets of standards.

Both sets of measurements were made using the same VNA (Agilent E8364C), controlled by PIMMS, and configured to measure in Ku-band waveguide from 12 GHz to 18 GHz in 0.1 GHz steps. The intermediate frequency (IF) bandwidth of the VNA was set to 10 Hz. An averaging factor of two was used during calibration and increased to eight for the DUT measurements. These IF bandwidth and averaging factor settings were chosen to achieve a good signal-to-noise ratio for the measurements. The calibration standards and DUTs were measured six times to provide an indication of the uncertainty in the measurements due to random effects.

Four DUTs were used for this comparison: (i) a near-matched load, (ii) an offset short-circuit, (iii) a 20 dB attenuator, and (iv) a 127 mm section of waveguide. These DUTs are typical of the types of device that are used to transfer metrological traceability at the NMI level. In addition, a mismatched load was measured. This particular device is measured every time PIMMS is used for measurements in Ku-band waveguide, and verifies the PIMMS measurements by comparison with measurements made on multiple previous occasions. The results for this verification device will be discussed in Section 6.

The results shown in the Figs. 7–10 include the measurement uncertainties expressed as 95% coverage intervals, at each measurement frequency, for both sets of measurements. Figs. 7 and 8 show the VRC measurements for the near-matched load and offset short-circuit, respectively, while Figs. 9 and 10 show the respective VTC measurements for the 20 dB attenuator and 127 mm section of waveguide. Since the two sets of uncertainties show considerable overlap in these Figures, it can be difficult to distinguish which uncertainties apply to which measurements. However, in each case, the tops and bottoms of the uncertainty bars follow the same shape as the lines that represent the measured values.

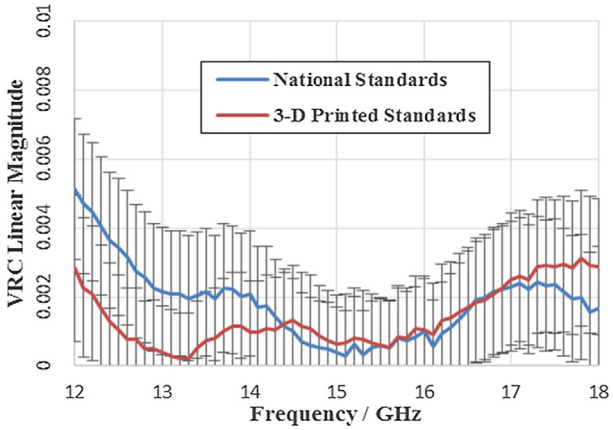

Fig. 7. VRC linear magnitude for the near-matched load.

The magnitude for both VRC and VTC data is presented in a linear format. The phase information for the VRC and VTC data is presented as the difference in phase between the two sets of measurements (i.e. using the 3-D printed standards and the UK's primary national standards). This is because the phase values vary significantly as a function of frequency and so it can be difficult to see differences between sets of phase measurements when presented as a function of frequency across the full waveguide band. These phase difference plots also show the uncertainty in the phase measurements. These uncertainties can be used to judge the significance of the difference in phase between the two sets of measurements – if the difference in phase is less than the combined phase uncertainty for both sets of measurements, then the difference is considered insignificant. The combined phase uncertainty, $U_c(f)$, is established at each frequency, f, using:

$$U_c(f) = \sqrt{U_1(f)^2 + U_2(f)^2} \tag{5}$$

where $U_1(f)$ and $U_2(f)$ are the frequency dependent uncertainties in the two sets of measurements.

Since the magnitude values for the near-matched load in Fig. 7 are very small, there is no benefit in comparing the measured

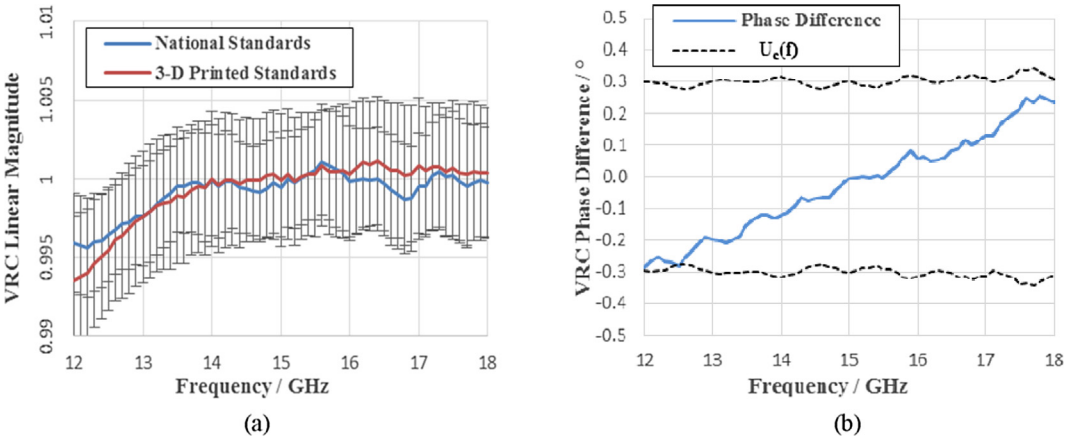

Fig. 8. VRC for the offset short-circuit: (a) linear magnitude; and (b) phase difference between the two sets of measurements.

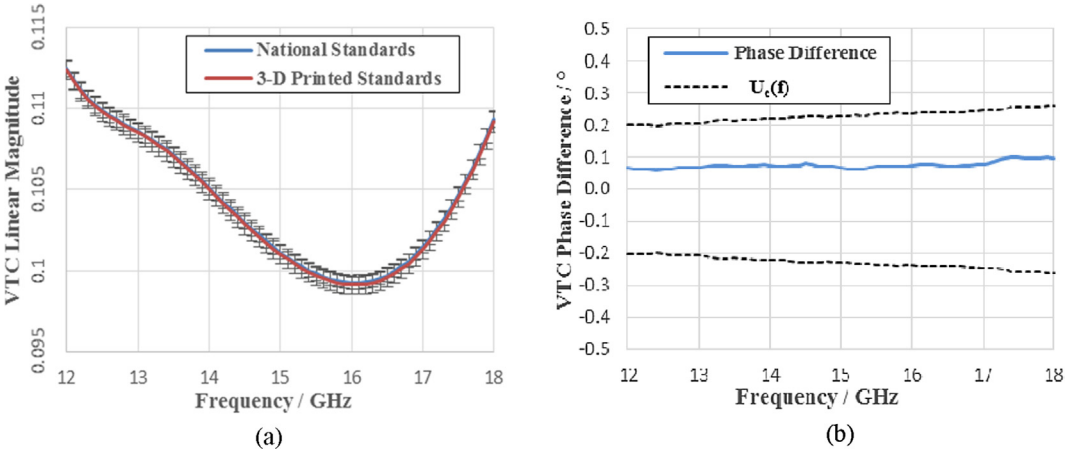

Fig. 9. VTC for the 20 dB attenuator: (a) linear magnitude; and (b) phase difference between the two sets of measurements.

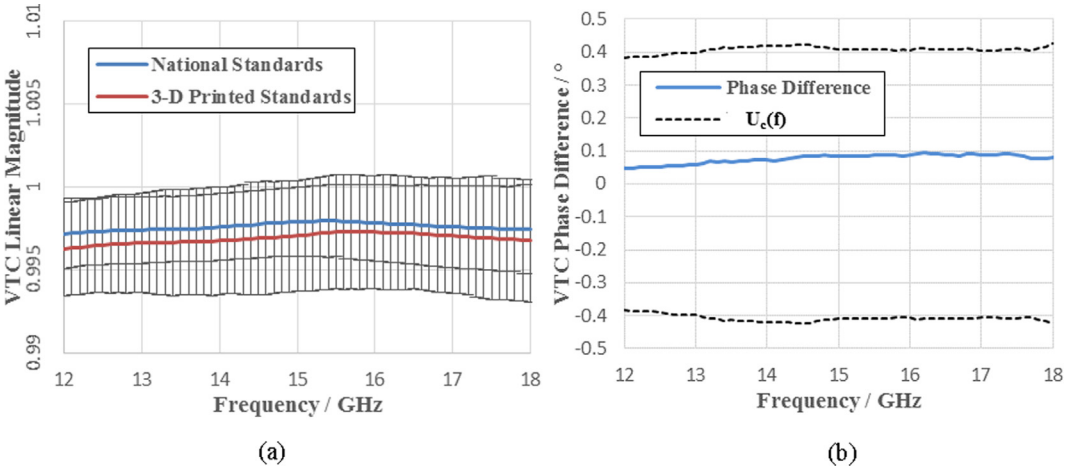

Fig. 10. VTC for the 127 mm section of line: (a) linear magnitude; and (b) phase difference between the two sets of measurements.

phase values for this device; in the limit, when the magnitude is zero, the phase is indeterminate. The magnitude values (in Figs. 7, 8(a), 9(a) and 10(a)) all show very good agreement between the two sets of measurements, with the uncertainty bars for both sets of measurements overlapping at all frequencies. The phase difference values (in Fig. 8(b), 9(b) and 10(b)) are all less than the associated combined uncertainty, indicating that the two sets of phase values are also in very good agreement.

This level of agreement between the two sets of measurements (i.e. made using the 3-D printed standards and the UK's primary national standards) demonstrates that these 3-D printed standards provide a similar level of performance as the UK's primary national

standards. This suggests that it is feasible to use 3-D printing techniques to manufacture waveguides of sufficient quality to be used as primary reference standards (e.g., by NMIs) to provide metrological traceability for S-parameters in waveguide at microwave frequencies.

5. VNA firmware comparison

The previous section demonstrated the 3-D printed devices being used as primary reference standards, in conjunction with a VNA, in a role that is performed by NMIs to confer metrological traceability to other laboratories. VNAs are also used extensively in many other roles, in both industry and academia. In fact, being so versatile, modern day VNAs can be used for just about every type of high-frequency electromagnetic measurement (which includes spectral analysis, nonlinear and time-domain network analysis) – in research, development, manufacturing and testing. In these scenarios, it is common to calibrate the VNA using standards that are already pre-characterised within the pre-installed VNA software; such 'firmware' calibrations are used by the vast majority of VNA end-users.

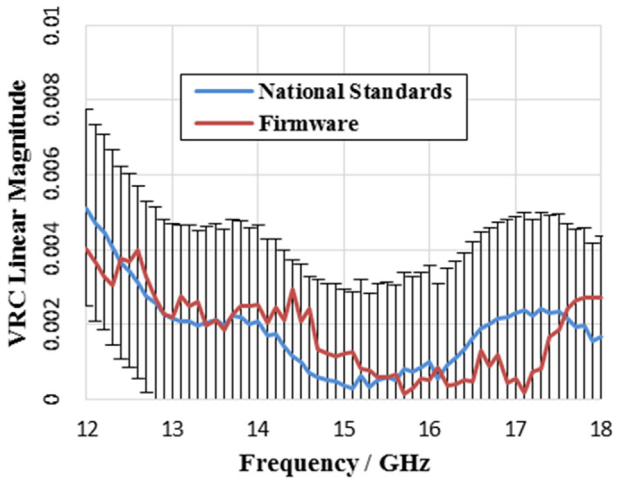

Fig. 11. VRC linear magnitude for the near-matched load. Measurements made using: 3-D printed standards with a VNA's firmware calibration and PIMMS using UK's primary national standards.

It is informative to investigate the quality of a VNA's firmware calibration, made using these 3-D printed standards. In order to do this, the characteristics of the standards are specified using the VNA firmware, prior to calibration [30]. The same DUTs as those measured in Section 4 were measured using the firmware calibration, so that the results could be directly compared with the same PIMMS measurements (made using the UK's primary national standards). Here, only uncertainties in the PIMMS national standard measurements are available, since a firmware VNA calibration does not evaluate the uncertainties in the measurements.

Figs. 11 and 12 show the results obtained for the near-matched load and the 20 dB attenuator. The level of agreement between the measurements made using the 3-D printed standards in conjunction with a VNA firmware calibration and the PIMMS national standard measurements is very good. The results for the other two DUTs (i.e., the offset short-circuit and 127 mm section of waveguide) showed similar very good agreement. This clearly demonstrates that these 3-D printed standards can be used successfully as standards when employing a VNA firmware calibration.

6. Discussion

All the results presented in Sections 4 and 5 demonstrate equivalence between measurements made with reference to the 3-D printed standards and the UK's primary national standards. Another important feature of measurement reliability is the ability to reproduce similar measurements made over an extended period of time. Such 'historical' measurement data is used at NPL to verify measurements made on any given occasion. To do this, the same device is measured each time that PIMMS is used in a given measurement configuration (e.g., for each coaxial and waveguide size supported by PIMMS). By comparing prior measurement data for the same device, the current measurement exercise can be verified. In the case of Ku-band waveguide, a mismatched load is used as the verification device.

Fig. 13 shows PIMMS measurement results using the UK's primary national standards, for the VRC of the mismatched load at 15 GHz, on five different occasions, in: 1996, 2002, 2007, 2014 and 2019. The 2019 values relate to the PIMMS measurement results presented in this paper, made using the UK's primary national standards. Fig. 13 also shows the PIMMS measurement results that were obtained in this paper using the 3-D printed standards; labelled "PIMMS (3-D printed)". Similarly, the results obtained using the 3-D printed standards in conjunction with a VNA firmware calibration are labelled "Firmware (3-D printed)".

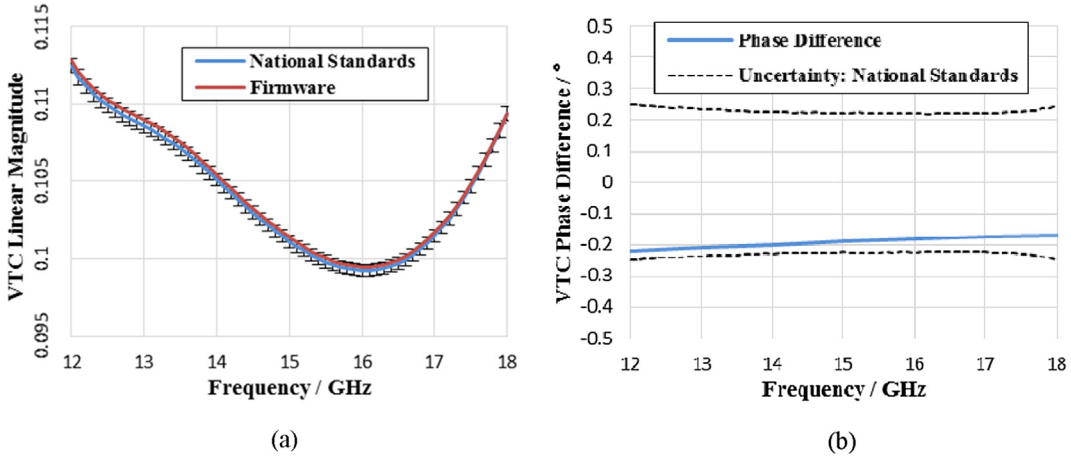

Fig. 12. VTC for the 20 dB attenuator. Measurements made using 3-D printed standards with a VNA's firmware calibration and PIMMS using the UK's primary national standards: (a) linear magnitude; and (b) phase difference.

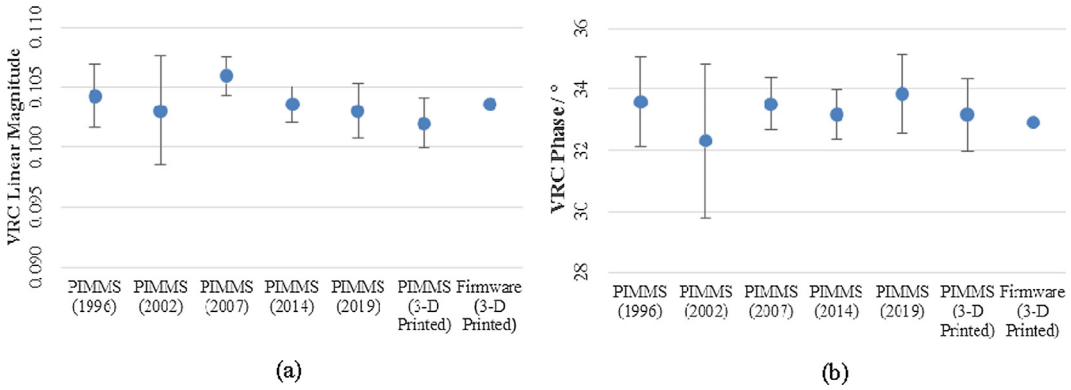

Fig. 13. Historical VRC measurement data for the mismatched load verification device at 15 GHz: (a) linear magnitude; and (b) phase.

From Fig. 13, it is clear that both sets of results obtained using the 3-D printed standards show very good agreement, for both VRC magnitude and phase, with the historical measurement data for this device (which covers a period of more than 20 years). This provides very good assurance that measurements made using the 3-D printed standards as calibration devices (either in conjunction with PIMMS or a VNA firmware calibration) are equivalent to measurements made using the UK's primary national standards as calibration devices, over an extended period of time.

7. Summary

This paper has demonstrated, for the first time, the feasibility of using 3-D printed devices as standards for calibrating VNAs at microwave frequencies. The measurement results achieved using these 3-D printed standards have shown very good agreement with measurements made using conventionally machined standards (i.e., the UK's primary national standards). This agreement has been shown when using the 3-D printed standards in conjunction with NPL's PIMMS (for NMI-level metrological traceability purposes) and when using a VNA's firmware calibration (as used by many VNA end-users).

The paper described the design and fabrication of the standards, followed by detailed assessments of the quality of the standards (using dimensional measurements and *in-operando* electrical assessments). The performance of these devices as calibration standards was assessed in terms of their use in conjunction with the UK's primary national standard system (PIMMS) and with a conventional VNA firmware calibration. In both cases, the standards demonstrated very good performance.

The bandwidth of these standards is constrained by the bandwidth of the rectangular waveguide, which is inherently narrow band. The bandwidth could be extended by choosing a different type of waveguide – e.g. ridged waveguide [31,32]. Although rectangular waveguides have been 3-D printed that operate at 1 THz [10], the current limits on this technology mean that these waveguides are not suitable as standards at these frequencies. However, work reported in [4] suggests that rectangular waveguide could be fabricated using 3-D printing techniques that could be used as standards to at least 100 GHz.

This work opens-up the possibility of institutions/end-users using 3-D printing techniques to fabricate their own calibration standards, rather than relying on the supply of such devices from manufacturers/vendors (who may not be easily accessible to the end-user, perhaps situated at a remote location). It also enables end-users to manufacture bespoke standards to meet particular applications where perhaps existing standards and metrological traceability may not exist (e.g., for other types of waveguide, such as circular and double-ridged waveguide, or rectangular waveguides in non-standard sizes for specialist applications such as radio astronomy). It should be noted that 3-D printing techniques are also well-suited for manufacturing structures that are not currently realisable using conventional 'subtractive' manufacturing techniques and so this could give rise to new types of waveguide geometry that currently do not exist, without having to wait for manufacturers to develop them.

If standards are fabricated by end-users, at end-user locations, then access to software that evaluates the uncertainty in the measurements [14–16] will enable metrological traceability to be demonstrated by these end-users, at their end-user locations. This could establish an entirely new approach for the dissemination and maintenance of metrological traceability to the International System of units (SI), by moving away from the reliance on manufacturers to supply standards and NMIs to supply traceability. This approach also aligns with plans by organisations such as the European Space Agency (ESA) for future non-terrestrial manufacturing strategies [33,34].

CRediT authorship contribution statement

Adam Jones: Formal analysis, Writing - review & editing. **Stepan Lucyszyn:** Investigation, Methodology, Writing - review & editing. **Enrique Márquez-Segura:** Conceptualization, Writing - review & editing. **Nick Ridler:** Conceptualization, Formal analysis, Writing - original draft. **James Skinner:** Formal analysis, Writing - review & editing. **Daniel Stokes:** Formal analysis, Writing - review & editing.

Declaration of Competing Interest

The authors declare that they have no known competing financial interests or personal relationships that could have appeared to influence the work reported in this paper.

Acknowledgement

This work was supported by the National Measurement System (NMS) Programme of the UK Government's Department for Business, Energy and Industrial Strategy (BEIS). The work was also supported by the Spanish Ministerio de Economía, Industria y Competitividad, under Project ADDMATE TEC2016-76070-C3-3-R (AEI/FEDER, UE), and by the Spanish Ministerio de Educación, Cultura y Deporte, under Grant PRX16/00358.

References

[1] B. Zhang, H. Zirath, Metallic 3-D printed rectangular waveguides for millimeter-wave applications, IEEE Trans. Compon. Packag. Manuf. Technol. 6 (5) (May 2016) 796–804.

[2] B. Zhang, Z. Zhan, Y. Cao, H. Gulan, P. Linner, J. Sun, T. Zwick, H. Zirath, Metallic 3-D printed antennas for millimeter- and submillimeter wave applications, IEEE Trans. Terahertz Sci. Technol. 6 (4) (July 2016) 592–600.

[3] C. Guo, X. Shang, M.J. Lancaster, J. Xu, A 3-D printed lightweight X-band waveguide filter based on spherical resonators, IEEE Microwave Wirel. Compon. Lett. 25 (7) (July 2015) 442–444.

[4] M. D'Auria, W.J. Otter, J. Hazell, B.T.W. Gillatt, C. Long-Collins, N.M. Ridler, S. Lucyszyn, 3-D printed metal-pipe rectangular waveguides, IEEE Trans. Compon. Packag. Manuf. Technol. 5 (9) (2015) 1339–1349.

[5] C. Guo, X. Shang, J. Li, F. Zhang, M.J. Lancaster, J. Xu, A lightweight 3-D printed X-band bandpass filter based on spherical dual-mode resonators, IEEE Microwave Wireless Compo. Lett. 26 (8) (2016) 568–570.

[6] X. Shang, P. Penchev, C. Guo, M.J. Lancaster, S. Dimov, Y. Dong, M. Favre, M. Billod, E. De Rijk, W–Band waveguide filters fabricated by laser micromachining and 3-D printing, IEEE Trans. Microw. Theory Tech. 64 (8) (2016) 2572–2580.

[7] B.T.W. Gillatt, M. D'Auria, W.J. Otter, N.M. Ridler, S. Lucyszyn, 3-D printed variable phase shifter, IEEE Microwave Wireless Compo. Lett. 26 (10) (2016) 822–824.

[8] X. Shang, P. Klasmann, M.J. Lancaster, A compact Ka-band waveguide orthomode transducer fabricated by 3-D printing, in: Proceedings of the 46th European Microwave Conference (EuMC), October 2016, pp. 365–368.

[9] W.J. Otter, S. Lucyszyn, Printing: the future of THz, IET Electron. Lett. 53 (7) (March 2017) 433.

[10] W.J. Otter, N.M. Ridler, H. Yasukochi, K. Soeda, K. Konishi, J. Yumoto, M. Kuwata-Gonokami, S. Lucyszyn, 3D printed 1.1 THz waveguides, IET Electron. Lett. 53 (7) (2017) 471–473.

[11] W.J. Otter, S. Lucyszyn, Hybrid 3-D-printing technology for tunable THz applications, in: Proceedings of the IEEE, Special Issue on Additive Manufacturing of Radio-Frequency Components, 105 (4) (2017) 756–767.

[12] B. Al-Juboori, J. Zhou, Y. Huang, M. Hussein, A. Alieldin, W.J. Otter, D. Klugmann, S. Lucyszyn, Lightweight and low-loss 3-D printed millimeter-wave bandpass filter based on gap-waveguide, IEEE Access 7 (1) (2018) 2624–2632.

[13] G.F. Engen, C.A. Hoer, Thru-Reflect-Line: an improved technique for calibrating the dual six-port automatic network analyzer, IEEE Trans. Microw. Theory Tech. 27 (12) (1979) 987–993.

[14] R.A. Dudley, N.M. Ridler, Traceability via the Internet for microwave measurements using vector network analysers, IEEE Trans. Instrum. Meas. 52 (1) (2003) 130–134.

[15] D.F. Williams, A. Lewandowski, NIST Microwave Uncertainty Framework, National Institute of Standards and Technology (NIST), USA, 2011. http://www.nist.gov/ctl/rf-technology/relatedsoftware.cfm.

[16] Wikipedia – The Free Encyclopaedia, List of uncertainty propagation software. https://en.wikipedia.org/wiki/List_of_uncertainty_propagation_software.

[17] IEC 60153-2:2016, Hollow metallic waveguides – Part 2: Relevant specifications for ordinary rectangular waveguides.

[18] IEEE Std 521-2002, IEEE Standard Letter Designations for Radar-Frequency Bands.

[19] E. Napadensky, H. Gothait, Three dimensional printing method and model obtained. European Patent Office EP1274551B1, 2001.

[20] "PSS_PJ_Objet260Connex3_0517a" Stratasys Ltd. Technical specification, 2016. https://www.stratasys.com/3d-printers/objet260-connex3.

[21] "MSS_PJ_DigitalABSPlus_0318a" Stratasys Ltd. Material data sheet, 2018. https://www.stratasys.com/materials/search/digital-abs-plus.

[22] A. Fares Karam, G. Stremsdoerfer, Plastics Metallization using a Dynamic Chemical Plating Process, in: K.L. Mittal (Ed.), Metallized Plastics 5&6: Fundamental and Applied Aspects, pp. 137–144, 1998.

[23] JCGM 100:2008, Evaluation of measurement data – Guide to the expression of the uncertainty in measurement, first ed., Bureau International des Poids et Measures (BIPM), September 2008. https://www.bipm.org/en/publications/guides/gum.html.

[24] N.M. Ridler, J.C. Medley, An uncertainty budget for VHF and UHF reflectometers, NPL Report DES 120, National Physical Laboratory (NPL), Teddington, UK, May 1992.

[25] N.M. Ridler, A review of existing national measurement standards for RF and microwave impedance parameters in the UK, IEE Colloquium Digest, No 99/008, pp 6/1-6/6, February 1999.

[26] The BIPM key comparison database (KCDB), Calibration and Measurement Capabilities – CMCs, Bureau International des Poids et Mesures (BIPM). https://kcdb.bipm.org/appendixC/.

[27] International Equivalence of Measurements: the CIPM Mutual Recognition Arrangement (MRA), Bureau International des Poids et Mesures (BIPM). https://www.bipm.org/en/cipm-mra/.

[28] N.M. Ridler, M.J. Salter, An approach to the treatment of uncertainty in complex S-parameter measurements, Metrologia 39 (3) (June 2002) 295–302.

[29] N.M. Ridler, M.J. Salter, Evaluating and expressing uncertainty in high-frequency electromagnetic measurements—a selective review, Metrologia 51 (2014) S191–S198.

[30] Specifying Calibration Standards and Kits for Keysight Vector Network Analyzers, Keysight Technologies Application Note, June 2016. http://literature.cdn.keysight.com/litweb/pdf/5989-4840EN.pdf.

[31] S. Hopfer, The design of ridged waveguides, IRE Transactions on Microwave Theory and Techniques, vol. 3, October 1955, pp. 20–29.

[32] MIL-W-23351/4C, Waveguides, Double Ridge (Bandwidth 2.4:1), January 2009.

[33] Building a lunar base with 3D printing. https://sservi.nasa.gov/articles/building-a-lunar-base-with-3d-printing/.

[34] Lunar 3D printing. http://www.esa.int/Highlights/Lunar_3D_printing.